Journal of Advanced Electrochemistry 2(1) (2016) 32–36

ISSN: 2455-0205

Contents List available at JACS Directory

Journal of Advanced Electrochemistry

journal homepage: http://www.jacsdirectory.com/jaec

Synthesis and Structural Transformation of [0.7(Ag_2CdI_4):0.3(AgI_x:$CuI_{(1-x)}$)] of Fast-Ion Conductor (x = 0.2, 0.4, 0.6 and 0.8 Mol. Wt. %)

Noorussaba, Ishaat M. Khan, A. Ahmad*

Solid State Chemistry Lab, Department of Chemistry, Aligarh Muslim University, Aligarh – 202 002, UP, India.

ARTICLE DETAILS

Article history:
Received 18 November 2015
Accepted 07 December 2015
Available online 14 December 2015

Keywords:
Fast-Ion Conductor
X- Ray Diffraction
Thermal Analysis
Doping

ABSTRACT

Some novel fast ionic solids in the mixed system were made to prepare [0.7(Ag_2CdI_4):0.3(AgI_x:$CuI_{(1-x)}$)] where x = 0.2, 0.4, 0.6 and 0.8 mol. wt. % respectively by solid state reaction and quenching them at particular temperature. Powdered samples of different compositions containing x mol. wt. % of (AgI_x:$CuI_{(1-x)}$) were synthesized by solid state reactions, using [Ag_2CdI_4] ternary halides as host. Powder specimens of these compositions were analyzed using differential thermal analysis (DTA), differential scanning calorimetry (DSC), thermal gravimetric analysis (TGA), Fourier transmission infrared spectra (FTIR) and x-ray powder diffraction (XRD) techniques. In host system, Ag and Cu substitution appears to stabilize the high-temperature, hexagonal structure to temperature well in excess of 445K, associated correspondingly with the melting of the (Ag^+:Cu^+) sublattice and with the storage of iodide/or cadmium sublattices.

1. Introduction

In recent years one can see an upsurge in the interest of researchers in solid state fast ion conductors such as A_2BX_4, etc. They presents a large group of A_2BX_4 compounds (A = Ag, Cu, B = Mg, Zn, Cd, Hg, Ge, Pb, and X = Cl, Br, I), which should be iso-structural or at least, reveal very similar structures [1]. Such fast ion conductors (i.e. Ag_2CdI_4) reveal attractive conductivity properties and represents meta-solid state fast ionic conductors [2]. This also arouses interest in their application for chemical sensors [3]. Due to their wide applications in solid state batteries and fuel cells, large numbers of researchers are working on their transport properties [4]. The design of electric batteries and potential optical devices requires an understanding of the role of the electronic structure in super ionic conductors [5]. One of the important aspects in understanding super ionic solids is the motion of mobile ions [6]. Several attempts have been made to synthesize new fast ionic solids suitable for electrochemical applications because of their high ionic conductivities at ambient temperatures, while characterization is an essential part in the development of new materials [7]. The new materials are linked by their high ionic conductivities; they display a wide variety of behavior in both the critical region and in the fast ion state [8]. Two routes can lead to improved solid fast ionic conductors, a search for new compounds and structures sustaining high level of ionic conductivity or a modification of existing compounds by heterogeneous or homogeneous doping [9]. Heterogeneous doping, on the contrary, involves mixing with a second phase with very limited solid solubility and for motion of defect concentration profiles in the proximity of interface, the deviation from local electrical neutrality (space charge) is a consequence of point defect equilibrium at interfaces [10]. A number of solids fast ionic conductors undergoa solid phase transition to a high temperature phase accompanied by a sharp jump in ionic conductivity by a factor of ~ 10^4 as well as a structural change [11]. Many fast ionic compounds including those belonging to the A_2BX_4 group (A = Ag and Cu, B = Cd and Hg, X = I) are usuallyobtained by means of ceramic technology [12-15]. Chemical substitution has been used extensively in recent years to modify either the magnitude of ionic conductivity or the transition temperature separating super ionic and covalent phases in various solid electrolytes [16]. Present work is based on the study of some nominal compositions of [0.7(Ag_2CdI_4):0.3(AgI_x:$CuI_{(1-x)}$)where x = 0.2, 0.4, 0.6 and 0.8 mol. wt. % respectively using the differential thermal analysis (DTA), differential scanning calorimetry (DSC), thermal gravimetric analysis (TGA), Fourier transmission infrared spectra (FTIR) and x-ray powder diffraction (XRD) techniques. Ag_2CdI_4 is hexagonal, with space group P6/mmm and unit cell dimensions a = 4.578 Å and c = 7.529 Å [17]. The solid fast ion conductors Ag_2CdI_4 exhibits a number of solid state phase transitions upon heating. Room temperature, covalent phase Ag_2CdI_4 crystallizes in a well-defined structure. Ag_2CdI_4 at T < 330 K belongs predominantly to hexagonal, with space group P6/mmm and unit cell dimensions a = 4.578 Å and c = 7.529 Å and changes to cubic at T > 380 K with space group Pm^3m and unit cell dimension a = 5.05 Å [18]. The temperature dependent thermochromism is due to changes in the charge transfer spectra arising from the donation of electron charge from the filled p-orbitals of the iodide ligands to the unfilled d-orbitals of the cadmium atom. The phase transition is considered to be an order-disorder type. The low temperature, β-phase for Ag_2CdI_4 are tetragonal but they differ in the placement of the A^+ cations and vacancy. In the high temperature, α- phase, the iodide sublattice is retained while cations are distributed randomly among all sites. Thus, (A_2BX_4) are isostructural in their α- phases, clearly, them, the A^+ cations plays a role in the exact structure in the low temperature form and determines, for the most part, the conductivity, phase transition temperature and thermo chromic properties [19]. We have undertaken a study of the synthesis and properties of the analogues of A_2BX_4 with the overall objective to fine tune the structural, spectral and thermal properties of Ag_2CdI_4 compounds with the choice of A^+ and possible mixed (Ag^+:Cu^+) substitutions to obtain materials useful for sensors and others electrochemical devices.

Although the initial purpose of this work is to see cations double (Ag^+:Cu^+) effect by introducing in A_2BX_4 systems, we find that it is quite difficult to see this and instead we find the structure of pure A_2BX_4 systems is different from iodide fast ionic system leading to the phase separation structure.

2. Experimental Methods

Silver tetraiodocadmiate [Ag_2CdI_4] was prepared from AgI and CdI_2 obtained from CDH (India) and LobaChemie, with stated purity of 99% and 99.2% respectively by the solid state reactions method. AgI and CdI_2 were mixed in the requisite composition in an agate mortar and were heated at 150 °C (423 K) for 5 days (120 h) in silica crucible with intermittent grinding. The rate of heating was initially kept at 50 °C per hour for 12 h.

*Corresponding Author
Email Address: afaqahmad21@gmail.com (Afaq. Ahmad)

Cite this Article as: Noorussaba, I.M. Khan, A. Ahmad, Synthesis and structural transformation of [0.7(Ag_2CdI_4):0.3(AgI_x:$CuI_{(1-x)}$)] of fast-ion conductor (x = 0.2, 0.4, 0.6 and 0.8 mol. wt. %), J. Adv. Electrochem. 2(1) (2016) 32–36.

After cooling, the dark lemony color compound changed to light lemony color. Ag_2CdI_4 is dark lemony yellow above 57-107 °C [20].

AgI and CuI were mixing in various x = 0.2, 0.4, 0.6 and 0.8 mol. wt. % respectively in an Agate motar to form (AgI_x:$CuI_{(1-x)}$) composite mixture by solid state reaction. Now Silver tetra-iodocadmiate 0.7 mol. wt. % [Ag_2CdI_4] were doped by 0.3 mol. wt. % (AgI_x:$CuI_{(1-x)}$) composite mixture to form [0.7(Ag_2CdI_4):0.3(AgI_x:$CuI_{(1-x)}$)] fast ion conductor, in an Agate mortar at room temperature and heating them at 200 °C (473 K) for 24 h in a silica crucible by procedures reported earlier [21]. After intermittent grinding, the powder mixture, were ground thoroughly in an agate mortar and collected in a silica crucible which is then kept in an air oven (CE 0434 NSW- 144) for 24 hours at 200 °C. The resulting powdered sample were pressed into pellets (2.4 cm diameter, 0.1 cm thick) by pouring the requisite amount of the compound into a stainless steel die using KBr at a pressure of 5 tons/cm^2 using a hydraulic press (Spectra Lab Model SL- 89). The IR spectrum was recorder for all the fast ionic composite systems [0.7(Ag_2CdI_4):0.3(AgI_x:$CuI_{(1-x)}$)] (where x = 0.2, 0.4, 0.6 and 0.8 mol. wt. % respectively) in the mid-infrared range 400-4000 cm^{-1} (25-25 μm) at room temperature using a INTERSPEC-2020, FTIR spectrophotometer measured in KBr [21].

The X-ray diffraction studies were performed for all the samples using Rigaku Rad B powder diffractometer with a K-beta filter with CuKα (λ = 1.54060 Å) radiation at room temperature. The angle range for measurement was 10 °C to 80 °C and the scanning speed was 1°/min.

DTA, DSC and TGA analysis were performed by Perkin Elmer Pyris Diamond model in nitrogen atmosphere (200 mL/min) at a heating rate of 5 °C per minute and a temperature range of 20 °C to 300 °C.

Differential thermal analysis (DTA) was performed by universal Schimadzu SC - TA-60 thermal analyzer equipped with disk memory and data analyzer in the temperature range 20–500 °C, with the powder sample sealed in pt capsules at heating rates of 10 °C min^{-1}/air medium. Differential scanning calorimetry (DSC) and Thermo-gravimetric analysis (TGA) were performed by DTG-60H thermal analyser in nitrogen atmosphere with flow rate of 30 mL min^{-1} and heating rate 25 °C min^{-1} in the temperature range 20-500 °C. The reference used was 10 mg alumina powder.

3. Results and Discussion

3.1 FTIR Analysis

3.1.1 FTIR Discussion in Ag_2CdI_4

As in Ketelaar description, the α- phase retains the same iodine structure as in the β phase. While the cation and vacancy sites becomes equivalent [1]. Later studies [2, 3] showed that the low temperature phases are tetragonal and in addition, are not isostructural, differing in the placement of the two monovalent cation (Ag or Cu) and vacancy. Thus based on data from the best single crystals, i.e. tetragonal β- phase was the only stable low-temperature phase and the apparent phase change after cycling could be explained by the formation of domains with the tetragonal c axis randomly oriented along the three spatial axes, thus giving the impression of a cubic lattice. The interpretation of a single low-temperature phase has the broadest base of support of the two views at present [3]. Assuming the β phase is tetragonal, the number and symmetry of normal modes can be determined. Group theory analysis finds the following number and symmetries for the 18 optical modes in Ag_2CdI_4 materials.

$$Ag_2CdI_4: 3A+ 5B+ 5E$$

The Infrared and Raman selection rules give the following allowed mode symmetries.

Infrared - Ag_2CdI_4: 5B+ 5E (10 Bands)
Raman - Ag_2CdI_4: 3A+ 5B+ 5E (13 Bands)

Using projection operators, we find that the B symmetry mode involve motion of the cation along the tetragonal c axis (z), and the E modes involve motion of the cations, along the a and b axes (x or y), B mode couple to electric fields along the z axis and E modes couple to fields in the xy plane, so that FTIR spectra would determine the mode-symmetry assignments uniquely [4-7].

3.1.2 Factor Group Analysis of Ag_2CdI_4

The irreducible representation for the 15 IR allowed modes are listed in Table 1. The unit cell group analysis of Ag_2CdI_4 is also shown in Table 1 [6], with the D_{2d} - S_4 correlation being A_1 and A_2 to A, B and B_2 to B and E to E. Fig. 1 shows FTIR spectrum for [0.7(Ag_2CdI_4):0.3(AgI_x:$CuI_{(1-x)}$)] fast ionic conductors where x = 0.2,0.4, 0.6 and 0.8 mol. wt. %.

In the IR spectra of [0.7(Ag_2CdI_4):0.3($AgI0_{.8}$:$CuI_{0.2}$] the 2351 cm^{-1} peak in Table 1 is strongest in xx, yy and zz direction making it an A. The A peak shifted in x = 0.4, 0.6 and 0.8 at 2322, 2244, 2389 cm^{-1}. The peak at 1460 cm^{-1} and 1396 cm^{-1} are strongest in the xx and yy polarizations and therefore belongs to A or B classes. This peak shifted in x = 0.4, 0.6 and 0.8 mol. wt. % composites are 1385 cm^{-1} for x = 0.4, 1385.01, 1333.42 cm^{-1} for x = 0.6 and 1508.02 cm^{-1} for x = 0.8 mol. wt. %. The only noticeable peaks in xz polarization and E symmetry is at 424 cm^{-1} and the 789 cm^{-1} shoulder appears to be weak in xx, zz and xz polarization making it likely that at least some of the peaks causing this feature would be maximized in the xy polarization and therefore of B symmetry in x = 0.2 mol. wt. %. E symmetry peaks are found in x = 0.4, 0.6 and 0.8 are at 416 cm^{-1}, 420.76 cm^{-1} and 440.60 cm^{-1}. The shoulder peaks appears in x = 0.4, 0.6 and 0.8 are 1083.43, 1000 and 1111.21 cm^{-1} respectively. The E peaks leaves some weak peaks at 464.40, 515.99 and 639.00 cm^{-1} in x = 0.2 which shifted in x = 0.4, 0.6 and 0.8 are at (460.44 cm^{-1}), (496.15 and 662.81 cm^{-1}) and (500.12 and 539.80 cm^{-1}) respectively.

Unassigned and a speculatively assignment for the 789 cm^{-1} feature. CdI_2 contamination peaks also found in at 623.13, 960, 662.81 and 539.80 cm^{-1} for x = 0.2, 0.4, 0.6 and 0.8 respectively. Peaks of B and E symmetry are allowed in the IR spectra and should be strong peaks. The occurrence of 422.66 cm^{-1} for [0.7(Ag_2CdI_4):0.3(AgI_{0x}:CuI_{1-x})] in the IR strengthens the E assignment for the peak at 424.72 cm^{-1}. For the x = 0.4, 0.6 and 0.8, the peaks are at 406.79, 419.79, 439 cm^{-1} in [0.7(Ag_2CdI_4):0.3(AgI_{0x}:CuI_{1-x})] respectively (Table 2).

Table 1 The irreducible representation for the 15 predicted modes of β- Ag_2CdI_4

	Ag_2CdI_4
Internal modes (HgI_4)	
Stretch	A+B+E
Deformation	
External modes (HgI_4)	
Rotatory	A+E
Translational	B+E
External Modes (Cu or Ag)	
Translational	B+E
Acoustic Modes	B+E

Table 2 [0.7(Ag_2CdI_4):0.3($AgI_{0.8}$:$CuI_{0.2}$] (wherex = 0.2,0.4, 0.6 and 0.8 mol. wt. %.) room temperature peaks and assignments.

[0.7(Ag_2CdI_4):0.3($AgI)_{(0.8)}$:$CuI_{(0.2)}$)]		[0.7(Ag_2CdI_4):0.3 ($AgI)_{(0.6)}$:$CuI_{(0.4)}$)]		[0.7(Ag_2CdI_4):0.3 ($AgI)_{(0.4)}$:$CuI_{(0.6)}$)]		[0.7(Ag_2CdI_4):0.3 ($AgI)_{(0.2)}$:$CuI_{(0.8)}$)]	
Peaks (cm^{-1})	Assign ments	Peaks (cm^{-1})	Assignm ents	Peaks (cm^{-1})	Assignm ents	Peaks (cm^{-1})	Assignm ents
2351	A	2322	A	2344	A	2389	A
1460	A	1385	A	1385	A	1508	A
789	?	1083	?	1000	?	1111	?
1396	B	-	B	1333	B	-	B
424	B_2	416	B	420.76	B	440.6	B

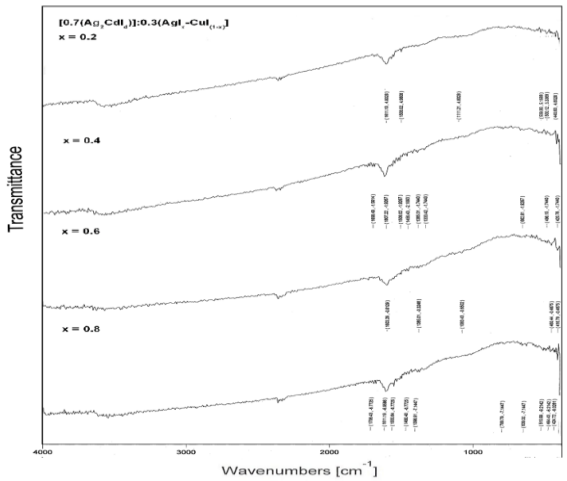

Fig. 1 FTIR spectrum for [0.7(Ag_2CdI_4):0.3(AgI_x:$CuI_{(1-x)}$)] fast ionic conductors, where (x = 0.2,0.4, 0.6 and 0.8 mol. wt. %).

3.1.3 FTIR Comparison in Ag_2CdI_4

From Table 3, the vibrational modes can be assigned by considering Ag_2CdI_4 as consisting of the vibrational modes of AgI and $(CdI_4)^{2-}$ species. In fact, as shown in Fig. 1, almost all the bands due to AgI and $(CdI_4)^{2-}$ are seen in the pure Ag_2CdI_4 composites. The band at 1601 cm^{-1} can be assignedto the symmetric stretching "A" mode of $(CdI_4)^{2-}$ species and this band is the strongest band at room temperature [11]. This assignment is

in good agreement with the other $(CdI_4)^{2-}$ tetrahedral compounds [12]. On the doping of $(Ag^+_{0.8}:Cu^+_{0.2})$ ions in the pure Ag_2CdI_4, all six bands shifted to 424, 464, 515, 639, 1556 and 1611 cm^{-1}. The 1000 - 1500 cm^{-1} region consists of two bands at the positions 1396 cm^{-1} and 1460 cm^{-1} at room temperature and at low temperature, these bands are expected to split.

Table 3 $[0.7(Ag_2CdI_4):0.3(AgI_x:CuI_{(1-x)})]$ fast ion conductors, where (x = 0.2, 0.4, 0.6 and 0.8 mol. wt. %), room temperature peaks and assignment.

Far-IR transmission peaks (cm^{-1})					Assignment
$[0.7(Ag_2CdI_4):0.3(AgI)_{(0.8)}:CuI_{(0.2)})]$	$[0.7(Ag_2CdI_4):0.3(AgI)_{(0.6)}:CuI_{(0.4)})]$	$[0.7(Ag_2CdI_4):0.3(AgI)_{(0.4)}:CuI_{(0.6)})]$	$[0.7(Ag_2CdI_4):0.3(AgI)_{(0.2)}:CuI_{(0.8)})]$	Symmetry	
440.60	496.15 420.76	460.44 416.79	515.99 464.40 424.72	A	Ag-I deformation
538.80 500.12	662.81	--------	639.00	A	Cd-I deformation
1111.21	1385.01 1333.42	1083.43	789.79	B	Cu-I symmetric stretch
1508.02	1456.43 1508.02	1385.01	1396.91 1460.40 1555.64	E	Ag-I symmetric stretch
1611.19	1607.22	1603.27	1611.19	E	$(CdI_4)^{2-}$- I symmetric stretch

It is known from the IR spectra of $(Ag^+_{0.8}:Cu^+_{0.2})$- ions conductors that this region consists of mostly of Ag-I [13] stretching modes. Hence, in all $[0.7(Ag_2CdI_4):0.3(AgI_x:CuI_{(1-x)})]$ composite samples, also the bands in this region can be assigned to symmetric stretching modes of Ag-I. Below 700 cm^{-1}, there are five sharp bands at 427, 449, 470, 493 and 520 cm^{-1} in pure Ag_2CdI_4 [11], while species vibrations, the bands at 424, 464, 515, 639 cm^{-1}, 416 and 460 cm^{-1}, 420, 496 and 662 cm^{-1} and 440, 500, 539, 477 cm^{-1} in x = 0.2, 0.4, 0.6 and 0.8 $(Ag^+:Cu^+)$-ions conductors respectively, it is known from factor group analysis studies [4] that the bands in this region are due to deformation type metal-iodine vibrations. On comparison with $(CdI_4)^{2-}$ species vibrations, the bands at 520 and 493 cm^{-1} in pure Ag_2CdI_4, and 639 cm^{-1} and 515 cm^{-1}, 662 cm^{-1} and 539 cm^{-1} and 612 and 532 cm^{-1} in x = 0.2, 0.6 and 0.8 $(Ag^+:Cu^+)$-ions conductors respectively (These bands are absent in x = 0.4 $(Ag^+:Cu^+)$-ions conductor) can be assigned to Cd-I deformation type bands. The band at 470 cm^{-1} in pure Ag_2CdI_4, and 464, 460, 496 and 500 cm^{-1} in x = 0.2, 0.4, 0.6 and 0.8 mol. wt. % $(Ag^+:Cu^+)$-doped ions conductors respectively, is attributed to the E symmetry of Ag^+ translational mode and is the characteristic attempt frequency of Ag^+ ion arising from the diffusive behavior to oscillatory behavior. This assignment is well explained by Shriver [7] by referring to the negative pressure dependence and also using theoretical calculations. The value assigned to the attempt frequencies in Ag_2CdI_4 is similar to cation transition modes in other related $(Ag^+:Cu^+)$-doped fast ionic conductors [7,11]. Another possibility is that motion of very large amplitude (diffusive like) is able to create configurationally disorder which allows all IR modes [14].

Inspection of Table 3 and Fig. 1, shows that IR spectra of all $[0.7(Ag_2CdI_4):0.3(AgI_x:CuI_{(1-x)})]$ and conductors exhibit the strongest feature at ca 1611.19, 1607.22, 1603.26 and 1611.19 cm^{-1} respectively, while the infrared activity below 900 cm^{-1} is weak. On the basis of the above discussion, these results strongly suggest that the existence of $(CdI_4)_2^{2-}/(Ag^+:Cu^+)$ tetrahedral in the x = 0.2 and 0.8 mol. wt. % $(Ag^+:Cu^+)$-doped fast ionic conductors should be excluded at least in concentration detectable by infrared spectroscopy.

Therefore, it is found that the infrared activity of the x = 0.2 and x = 0.8mol. wt. % $(Ag^+:Cu^+)$-fast ionic conductors arises from $(CdI_4)^{2-}$ tetrahedral, while x = 0.4 mol. wt. % $(Ag^+:Cu^+)$-fast ionic conductors show weakest feature at lower frequencies. Increasing the $Ag^+:Cu^+$ content induces a decreases to increase of the infrared activity in $[0.7(Ag_2CdI_4):0.3(AgI_x:CuI_{(1-x)})]$ [11].

3.2 X-Ray Diffraction

Fig. 2 shows the typical XRD diffractogram obtained for Ag_2CdI_4 ternary halides doped with different compositions of $[0.7(Ag_2CdI_4):0.3(AgI_x:CuI_{(1-x)})]$ composites (where x = 0.2, 0.4, 0.6 and 0.8 mol. wt. %). In γ-AgI, iodide ions are known to form a mixture of close packed structures, at temperatures well below 420K (140 °C) consisting of fcc and hcp structures which are commonly designated as γ-AgI and β-AgI respectively. However, for pedagogical reasons only γ-AgI is considered at room temperature. According, to the xrd data obtained during the present study have been compared with that of γ-AgI. It is clear from Table 4 that all the xrd data contain 2θ values different from that of the starting materials. Also it is obvious from Table 4, that the above compositions are polycrystalline in nature consisting of a multiphase mixture of AgI phases. These phases have been identifies as follows.

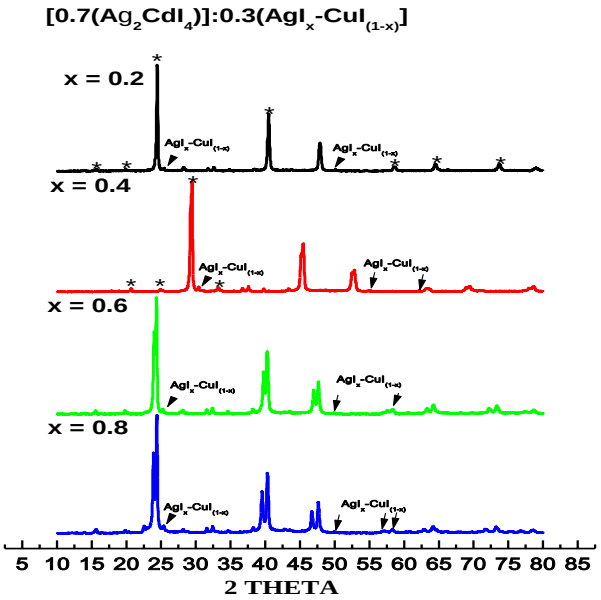

Fig. 2 X-ray diffractogram for $[0.7(Ag_2CdI_4):0.3(AgI_x:CuI_{(1-x)})]$ fast ion conductors

Table 4 X-ray diffractogram peaks and assignment for $[0.7(Ag_2CdI_4):0.3(AgI)_x:CuI_{(1-x)})]$ fast ion conductors

$[0.7(Ag_2CdI_4):0.3(AgI)_{(0.8)}:CuI_{(0.2)})]$		$[0.7(Ag_2CdI_4):0.3(AgI)_{(0.6)}:CuI_{(0.4)})]$		$[0.7(Ag_2CdI_4):0.3(AgI)_{(0.4)}:CuI_{(0.6)})]$		$[0.7(Ag_2CdI_4):0.3(AgI)_{(0.2)}:CuI_{(0.8)})]$	
2θ	Peak Assignment	2θ	Peak Assignment	2θ	Peak Assignment	2θ	Peak Assignment
15.74	Very short CuI	19.02	γ-AgI	43.53	γ- CuI	22.61	γ- CuI
20.04	Very short AgI	30.52	metallic silver	49.95	γ- CuI	44.66	γ- CuI
24.34	$CuIAg_2CdI_4$	64.21	metallic silver	58.24	γ- CuI	76.80	$CuIAg_2CdI_4$
25.45	AgI			64.19	$CuIAg_2CdI_4$		
28.33	CuI			73.35	$CuIAg_2CdI_4$		
31.70	$AgIAg_2CdI_4$						
32.62	AgI						
34.77	Ag_2CdI_4						
38.45	Ag_2CdI_4						
40.60	$CuIAg_2CdI_4$						
47.80	AgI						
58.55	Ag_2CdI_4						
64.38	Ag_2CdI_4						
73.59	Ag_2CdI_4						

3.2.1 $[0.7(Ag_2CdI_4):0.3(AgI_{0.8}:CuI_{0.2})]$-Doped Composites (where x = 0.2, 0.4, 0.6 and 0.8 mol. wt. %)

In case of $[0.7(Ag_2CdI_4):0.3(AgI_{0.8}:CuI_{0.2})]$-doped composites system, the peaks at 20.04°, 25.45°, 32.62° and 47.80° can be attributed to the presence of γ-AgI, whereas peaks observed at 24.34° and 40.60° have been compared with that of $CuIAg_2CdI_4$. In addition, γ-CuI lines have also been observed at 15.74° and 28.33°. Effectively the composition of $[0.7(Ag_2CdI_4):0.3(AgI_{0.8}:CuI_{0.2})]$-doped composites system consists of γ-AgI, $CuIAg_2CdI_4$, γ-CuI, $AgIAg_2CdI_4$, and pure Ag_2CdI_4 phases [22].

3.2.2 $[0.7(Ag_2CdI_4):0.3(AgI_{0.6}:CuI_{0.4})]$-Doped Composites (where x = 0.2, 0.4, 0.6 and 0.8 mol. wt. %)

In case of $[0.7(Ag_2CdI_4):0.3(AgI_{0.6}:CuI_{0.4})]$-doped composites system, the peaks observed at 19.02°, 31.21°, 22.94° and 23.22° alone could be attributed to the presence of γ-AgI in $[0.7(Ag_2CdI_4):0.3(AgI_{0.6}:CuI_{0.4})]$. Another interesting feature of this particular compositions is that the xrd pattern is quite broad in shape thus suggesting its highly disordered nature. However, small traces of silver aggregates may be present in this composite material. Since very faint lines observed at 30.52° and 62.21° could only be attributed to the presence of small traces of metallic silver in Ag_2CdI_4 (Table 4) [22].

Cite this Article as: Noorussaba, I.M. Khan, A. Ahmad, Synthesis and structural transformation of $[0.7(Ag_2CdI_4):0.3(AgI_x:CuI_{(1-x)})]$ of fast-ion conductor (x = 0.2, 0.4, 0.6 and 0.8 mol. wt. %), J. Adv. Electrochem. 2(1) (2016) 32–36.

3.2.3 [0.7(Ag_2CdI_4):0.3($AgI_{0.4}$:$CuI_{0.6}$)]-Doped Composites (where x = 0.2, 0.4, 0.6 and 0.8 mol. wt. %)

The xrd data corresponding to the composition having ($AgI_{0.4}$:$CuI_{0.6}$)]-doped composites of Ag_2CdI_4 system appears to suggest that γ-CuI may be the major content in the dopant materials because of the fact that lines observed at 2θ = 43.53°, 49.95° and 58.24° could befittingly attributed to the presence of γ-CuI. However, peaks observed at 2θ = 64.19° and 73.35° can be attributed to the presence of $CuIAg_2CdI_4$ as a constituent in the multiphase system (Table 4) [22].

3.2.4 [0.7(Ag_2CdI_4):0.3($AgI_{0.2}$:$CuI_{0.8}$)]-Doped Composites (where x = 0.2, 0.4, 0.6 and 0.8 mol. wt. %)

In case of the sample having [0.7(Ag_2CdI_4):0.3($AgI_{0.2}$:$CuI_{0.8}$)]-doped composites system, the observed xrd peaks at 22.61° and 44.66° may be attributed to the formation of CuI while the peak at 76.80° could be attributed to the presence of $CuIAg_2CdI_4$. Remaining unidentified peaks may be due to the presence of certain silver based compounds. From the above xrd analysis it is clear that all composite fast ionic conductors have been formed during the present investigation (Table 4).

3.3 Thermal Analysis

3.3.1 Differential Scanning Calorimetry

Fig. 3 depicts the DSC thermograms recorded for the sixteen different samples in the mixed fast ionic composite systems [0.7(Ag_2CdI_4):0.3(AgI_x:$CuI_{(1-x)}$)] (where x = 0.2, 0.4, 0.6 and 0.8 mol. wt. %).

It is clear from Fig. 4 and Table 5, that endothermic peaks are observed for [0.7(Ag_2CdI_4):0.3($AgI_{0.2}$:$CuI_{0.8}$)] composite, exhibits three endothermic peaks at 365.87 K, 493.69 K and 527.87 K, that can be assigned to the partial decomposition of ε-Ag_2CdI_4 in AgI, CdI_2 and β-Ag_2CdI_4 [23], γ-α phase transition of CuI (at 493.69 K), tends to notify the presence of AgI [24]. On the other hand the endothermic peak that appears at 527.87 K in the case of x = 0.2 mol. wt. % composition is found to compare well with the observed melting temperature of $CuIAg_2CdI_4$ composite [25]. The β-Ag_2CdI_4 peaks also occurs at 368.73 K, 372.75 K and 378.37 K in x = 0.4, 0.6 and 0.8 mol. wt. % respectively. This transition increases on further doping. The γ-α–CuI transition occurs at 493.31 K in x = 0.4, where γ-β-phase transition of AgI occurs at (478.04 K, 461.145 K) in DSC plot of x = 0.6 and 0.8 mol. wt. %.

The endothermic peaks occurs at 516.6 K in the case of x = 0.4 for $CuIAg_2CdI_4$ composites, whereas in x = 0.6, 0.8 mol. wt. %., the endothermic peaks appeared at 586.82 K, 494.84 K is found to compare well with the observed melting temperature of $AgIAg_2CdI_4$ composites. A careful analysis of the xrd patterns in Fig. 2 also reveals the formation of various other phases apart from Ag_2CdI_4, AgI or CuI. Therefore, the DSC results have indicated the presence of major content phases in [0.7(Ag_2CdI_4):0.3(AgI_x:$CuI_{(1-x)}$)] composite.

On the other hand the exothermic peaks obtained in DSC curves of all the composites are at 423 K, 453 K, 463.31 K and 463 K respectively. Clearly, the above mentioned exothermic peaks are comparable to that of β-α phase transition of pure AgI (≈420 K). The DSC results therefore suggest that the combination of the two starting materials namely (AgI:CuI) and Ag_2CdI_4 is complete for a composition around 50 mol. % Ag_2CdI_4 resulting in the formation of new substances which are probably Ag^+ ion conductors having very small traces of AgI [26].

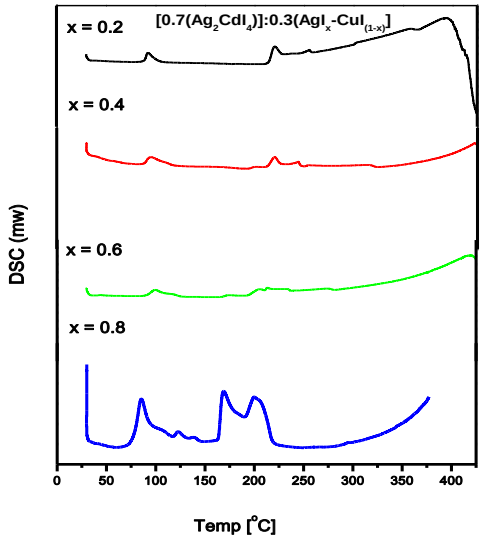

Fig. 3 DSC for [0.7(Ag_2CdI_4):0.3(AgI_x:$CuI_{(1-x)}$)] fast ionic conductors, (where x = 0.2,0.4, 0.6 and 0.8 mol. wt. %).

Table 5 DSC endothermic peaks for [0.7(Ag_2CdI_4):0.3(AgI_x:$CuI_{(1-x)}$)] fast ionic conductors (where x = 0.2,0.4, 0.6 and 0.8 mol. wt. %)

Composition	Endothermic Peaks (K)		
	I	II	III
[0.7(Ag_2CdI_4):0.3(AgI)$_{(0.2)}$:$CuI_{(0.8)}$)]	365.87	493.69	527.87
0.7(Ag_2CdI_4):0.3(AgI)$_{(0.4)}$:$CuI_{(0.6)}$)]	368.73	493.31	516.6
[0.7(Ag_2CdI_4):0.3(AgI)$_{(0.6)}$:$CuI_{(0.4)}$)]	372.75	478.04	586.82
[0.7(Ag_2CdI_4):0.3(AgI)$_{(0.8)}$:$CuI_{(0.2)}$)]	105.37	461.14	494.84

3.3.2 Differential Thermal Analysis

DTA curves for all the sixteen samples composition [0.7(Ag_2CdI_4):0.3(AgI_x:$CuI_{(1-x)}$)], are shown in Fig. 4. On comparing these curves, we note the following important features.

1. A well-defined intense peak prepared at ~353-393 K in all curves. This peak corresponds to a β-α- like transition of the host [Ag_2CdI_4]. The peak strength has increased on further doping of x mol. wt. % of (AgI:CuI). This is indicative of partial and complete stabilization of the high conducting α- like phase of the host [27] in the samples respectively. These observations are exactly correlate our DSC results.
2. A second intense and well defined peak appeared at ~453-493 K in all the DTA curves of [0.7(Ag_2CdI_4):0.3(AgI_x:$CuI_{(1-x)}$)] system. This peak obviously corresponds to the β–α like transition of CuI-AgI solid solutions, while in the DTA curves of Ag_2CdI_4 this peak occurs at around ~513-553 K. This β–α phase transition peak becomes broad with (AgI_x:$CuI_{(1-x)}$) content, this is due to the form of crystalline phase within space charge layer that is expected to form between (AgI:CuI) and [Ag_2CdI_4] (where x = 0.2,0.4, 0.6 and 0.8 mol. wt. %) [28].
3. It has been observed from the DTA curves of [0.7(Ag_2CdI_4):0.3(AgI_x:$CuI_{(1-x)}$)], that an additional peak is obtained after the β–α phase transition peak with the addition of (AgI_x:$CuI_{(1-x)}$) and its intensity increase with the mole fraction of (AgI:CuI). This peak attributed to interface interactions between (AgI_x:$CuI_{(1-x)}$) and [Ag_2CdI_4] (where x = 0.2, 0.4, 0.6 and 0.8 mol. wt. %).The above results clearly reveal the partial presence of fast ionic phase in all the samples.

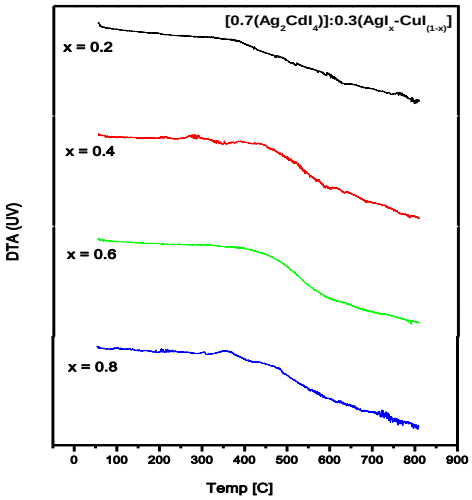

Fig. 4 DTA for [0.7(Ag_2CdI_4):0.3(AgI_x:$CuI_{(1-x)}$)] fast ionic conductors(where x = 0.2,0.4, 0.6 and 0.8 mol. wt. %).

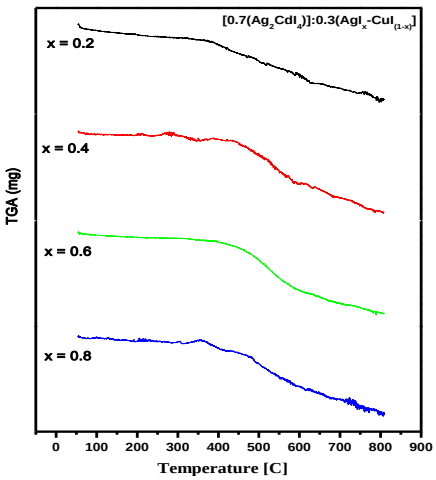

Fig. 5 TGA for [0.7(A_2BX_4):0.3(AgI_x:$CuI_{(1-x)}$)] fast ionic conductors, where (where A_2BX_4 = Ag_2CdI_4, Cu_2CdI_4, Ag_2HgI_4 and Cu_2HgI_4, x = 0.2,0.4, 0.6 and 0.8 mol. wt. %)

Cite this Article as: Noorussaba, I.M. Khan, A. Ahmad, Synthesis and structural transformation of [0.7(Ag_2CdI_4):0.3(AgI_x:$CuI_{(1-x)}$)] of fast-ion conductor (x = 0.2, 0.4, 0.6 and 0.8 mol. wt. %), J. Adv. Electrochem. 2(1) (2016) 32–36.

3.3.3 TGA Analysis

TGA curves for (AgI_x:$CuI_{(1-x)}$)-doped host samples, it shifts to a lower temperature because of the interaction between dopant (AgI_x:$CuI_{(1-x)}$) and host [Ag_2CdI_4] (where x = 0.2, 0.4, 0.6 and 0.8 mol. wt. %). In the TGA curves of [0.7(Ag_2CdI_4):0.3(AgI_x:$CuI_{(1-x)}$)] (Fig. 5), from room temperature up to about 400 °C. One distinct peak of TGA are obtained for the [0.7(Ag_2CdI_4):0.3(AgI_x:$CuI_{(1-x)}$)], in the temperature range 400–500 °C with corresponding mass loss for pure samples, and for (AgI_x:$CuI_{(1-x)}$)-doped host samples [29] are shown. These data corroborate the observations of TGA studies.

4. Conclusion

A novel composite fast ion conductors [0.7(Ag_2CdI_4):0.3(AgI_x:$CuI_{(1-x)}$)] where x = 0.2, 0.4, 0.6 and 0.8 mol. wt. % respectively by solid state reaction. Powdered samples of different compositions containing x mol. wt. % of (AgI_x:$CuI_{(1-x)}$) were synthesized by solid state reactions, using [Ag_2CdI_4] ternary halides as host. In addition, Ag and Cu substitution appears to stabilize the high-temperature, hexagonal structure to temperature well in excess of 445K, associated correspondingly with the melting of the (Ag^+:Cu^+) sublattice and with the storage of iodide /or cadmiumsublattices.

Fourier transmission infrared spectra of all the fast ionic conductors [0.7(Ag_2CdI_4):0.3(AgI_x:$CuI_{(1-x)}$)] (where x = 0.2, 0.4, 0.6 and 0.8 mol. wt. %) in the wavenumber range extending from 400 to 4000 cm^{-1} are also reported.

X-ray powder diffraction, DTA, DSC and TGA studies confirmed the formation of a superionic phase in the composite system. The temperature dependence of various ionic parameters was determined to characterize the ion transport properties and doping effect.

Acknowledgements

The authors are gratefully acknowledged to UGC, New Delhi, India for financial assistance as UGC-PDF Women Scientist Scheme. The authors gratefully acknowledge Prof. Reshef Tenne and Dr. Feldmann at the Wiezmann Institute of Science (Israel) for obtaining the x-ray measurements of our pure samples. The authors also gratefully acknowledge the Chairman of the Department of Chemistry for providing the research facilities.

References

[1] H.W. Zandbergen, The crystal structure of α-thallium hexaiodochromate, α - Tl_4CrI_6, Acta Cryst. B. 35 (1979) 2852-2855.
[2] A.V. Franiv, O.S. Kushnir, I.S. Girnyk, V.A. Franiv, I. Kityk, M. Piasecki, K.J. Plucinski, Growth and optical anisotropy of Tl_4CdI_6 single crystals, Ukr. J. Opt. 14 (2013) 6-13.
[3] D.S. Kalyagin, Y.E. Ermolenko, Y.G. Vlasov, Diffusion of Tl-204 isotope and ionic conductivity in Tl_4HgI_6 membrane material for chemical sensors, Rus. J. Appld. Chem. 81 (2008) 2172-2174.
[4] M. Hassan, M.S. Nawaz, Rafiuddin, Ionic conduction and effect of immobile cation substitution in binary system (AgI) 4/5–(PbI_2) 1/5, Radiat. Eff. Defect. S. 163 (2008) 885-891.
[5] K. Wakamura, Characteristic properties of dielectric and electronic structures in super ionic conductors, Solid State Ionics 149 (2002) 73–80.
[6] R. Sudharsanan, T.K.K. Srinivasan, Radhakrishna, Raman and far IR studies on Ag_2CdI_4 and Cu_2CdI_4 superionic compounds, Solid State Ionics 13 (1984) 277-283.
[7] A. Viswanathan, S. Austin Suthanthiraraj, Impedance and modulus spectroscopic studies on the fast ion conducting system CuI-Ag_2MoO_4, Solid State Ionics 62 (1993) 79-83.
[8] H.G. LeDuc, L.B. Coleman, Far-infrared studies of the phase transition and conduction mechanism in the fast-ion conductors Ag_2HgI_4 and Cu_2HgI_4, Phys. Rev. B 31 (1985) 933-941.
[9] P. Knauth, Ionic conductor composites: Theory and materials, Jour. Electroceram. 5 (2000) 111-125.
[10] J. Mair, Ionic conduction in space charge regions, Prog. Solid State Chem., Bull. Mater. Sci. 23 (1995) 171-263.
[11] E.A. Secco, A. Sharma, Structure stabilization: locking-in fast cation conductivity phase in TlI, J. Phys. Chem. Sol. 2 (1995) 251–254.
[12] J.B. Goodenough, Ceramic solid electrolytes, Solid State Ionics 94 (1997) 17-25.
[13] S. Beg, N.A.S. Al-Areqi and S. Haneef, Study of phase transition and ionic conductivity changes of Cd-substituted $Bi_4V_2O_{11-\delta}$, Solid State Ionics 179 (2008) 2260–2264.
[14] E. Kartini, T. Sakuma, K. Basar, M. Ihsan, Mixed cation effect on silver–lithium solid electrolyte $(AgI)_{0.5}(LiPO_3)_{0.5}$, Solid State Ionics 179 (2008) 706–711.
[15] R.C. Agrawal, R.K. Gupta, Superionic solid: composite electrolyte phase–an overview, J. Mater. Sci. 6 (34) (1995) 1131-1162.
[16] M.S. Kumari, E.A. Secco, Order-disorder transitions: solid state kinetics, thermal analysis, x-ray diffraction and electrical conductivity studies in the Ag_2SO_4-K_2SO_4 system, Can. J. Chem. 63 (1985) 324-328.
[17] V. Fernandez, F. Jaque, J.M. Calleja, Raman and optical absorption spectroscopic study of the thermochromic phase transition of Ag_2HgI_4, Solid State Commun. 59 (1986) 803-807.
[18] R.D. Shannon, Crystal physics, diffraction, theoretical and general crystallography, Acta Cryst. A 32 (1976) 751-767.
[19] H.H. Hofer, W. Eysel, U.V. Alpen, Electrochemistry of Na_2SO_4 (I) solid solutions with aliovalent cation substitution, Solid State Chem. 36 (1981) 365-370.
[20] K. Siraj, Rafiuddin, Study of ionic conduction and dielectric behavior of pure and K^+ doped Ag_2CdI_4, Soft Nanosci. Lett. 2 (2012) 13-16.
[21] R.C. Agrawal, R. Kumar, A. Chandra, Transport studies on a new fast silver ion conducting system: 0.7[0.75AgI:0.25AgCl]:0.3 [yAg_2O:(1– y)B_2O_3], Solid State Ionics 84 (1996) 51-60.
[22] A. Adamski, Z. Sojka, K. Dyrek, M. Che, An XRD and ESR study of V_2O_5/ZrO_2 catalysts: Influence of the phase transitions of ZrO_2 on the migration of V^{4+} ions into zirconia, Solid State Ionics 117 (1999) 113-122.
[23] E.A. Secco, M.G. Usha, Cation conductivity in mixed sulfate-based compositions of Na_2SO_4, Ag_2SO_4, and Li_2SO_4, Solid State Ionics 68 (1994) 213-219.
[24] Noorussaba, A. Ahmad, Composition-induced phase transition in a [Ag_2Hg1_4:0.2AgI] mixed composite system doped with CuI, Cen. Europ. J. Chem. 8(6) (2010) 1227-1235.
[25] R.C. Agrawal, R.K. Gupta, R. Kumar, A. Kumar, Ionic transport in the (AgI:AgCl) mixed-system, J. Mater. Sci. 29 (1994) 3673-3677.
[26] U. Lauer, J. Maier, Conductivity enhancement and microstructure in AgCl/AgI composites, Solid State Ionics 51 (1992) 209-213.
[27] Agrawal, M.L. Verma, R.K. Gupta, Electrical and electrochemical properties of a new silver, tungstate glass system: x[0.75AgI:0.25AgCl]:(1-x)[Ag_2O: WO_3], Solid State Ionics 171 (2004) 199–205.
[28] S. Sultana, R. Rafiuddin, Enhancement of ionic conductivity in the composite solid electrolyte system: TlI–Al_2O_3, Ionics 15 (2009) 621-625.
[29] A. Phukan, J.N. Ganguli, D.K. Dutta, $ZnCl_2$-Zn^{2+}-Montmorillonite composite: efficient solid acid catalyst for benzylation of benzene, J. Mol. Catal. A: Chem. 202 (2003) 279–287.